Atmospheric Environment 72 (2013) 165–170

Contents lists available at SciVerse ScienceDirect

Atmospheric Environment

journal homepage: www.elsevier.com/locate/atmosenv

Heterogeneous photochemical reaction of ozone with anthracene adsorbed on mineral dust

Jinzhu Ma, Yongchun Liu, Qingxin Ma, Chang Liu, Hong He*

Research Center for Eco-Environmental Sciences, Chinese Academy of Sciences, Beijing 100085, China

HIGHLIGHTS

- Reactions of O_3 with anthracene on TiO_2 and Asian dust were photo-enhanced.
- Anthraquinone can react with O_3 quickly in the presence of light.
- Reactions of O_3 with anthracene adsorbed on Asian dust proceed by the L–H mechanism.

ARTICLE INFO

Article history:
Received 31 October 2012
Received in revised form
14 January 2013
Accepted 24 February 2013

Keywords:
Anthracene
TiO_2
Asian dust storm particles
Ozone
Heterogeneous photochemical reactions
Kinetics

ABSTRACT

The heterogeneous reactions of O_3 with anthracene adsorbed on TiO_2 and on Asian dust storm particles were investigated in the dark and in the presence of light. The reaction rate constants of the heterogeneous reaction between O_3 and anthracene adsorbed on TiO_2 were increased by a factor of 1.5 in the presence of light compared to the dark conditions. Anthraquinone, which was identified as the main surface product of anthracene reacted with O_3 in the dark, can react with O_3 quickly in the presence of light. The reactions on Asian dust storm particles exhibited pseudo-first-order kinetics for anthracene loss, and the reactions between O_3 and anthracene adsorbed on Asian dust storm particles proceed by the Langmuir–Hinshelwood mechanism in the dark and in the presence of light. At extremely high ozone concentrations, the degradation of anthracene is enhanced by a factor of 3 in the presence of light compared to the dark conditions.

1. Introduction

Polycyclic aromatic hydrocarbons (PAHs) are mainly originated from the incomplete combustion of fossil fuels (petroleum, natural gas and coal) and biomass burning. Because of the high allergenic, mutagenic, and carcinogenic properties of PAHs (Finlayson-Pitts and Pitts, 1997), their transport and transformation in the environment attracted considerable interest over the past several decades (Bernstein et al., 1999; Fioressi and Arce, 2005; Fox and Olive, 1979; Matsuzawa et al., 2001; Pitts et al., 1980). Photolysis and ozonation are the most important transformation pathway for most PAHs adsorbed on natural substrates in the environment.

Photolysis of PAHs led to the formation of photo-oxidation products and photodimers (Barbas et al., 1994; Dabestani et al., 1995). Photochemical behaviours of PAHs are dependant not only on their molecular structures but also the physical–chemical properties of the substrate on which they are adsorbed. Carbonaceous particles can inhibit the photoreactivity of PAHs, while mineral particles can accelerate the photoreactivity of PAHs (Behymer and Hites, 1985; Dunstan et al., 1989; Korfmacher et al., 1980; Wang et al., 2005).

PAHs ozonation has been investigated on a variety of substrates, including phenylsiloxane oil (Kwamena et al., 2007), soot (Pöschl et al., 2001), azelaic acid (Kwamena et al., 2004), octanol and decanol (Kahan et al., 2006), NaCl (Gloaguen et al., 2006), pyrex glass (Kwamena et al., 2006), different coated aqueous surfaces (Mmereki et al., 2004) and mineral oxides (Ma et al., 2010). Under dark conditions, the rate of ozonation is highly influenced by the nature of the substrate and on the dispersion of the PAHs over the surface. These reactions proceed by a Langmuir–Hinshelwood mechanism, in which ozone adsorbs to the surface prior to reaction and the rate of reaction is dependant upon the surface concentration of PAHs and ozone.

To date, only a few studies have investigated the effect of solar radiation upon the heterogeneous ozonation of PAH adsorbed on solid surfaces (Cope and Kalkwarf, 1987; Prokopenko and Osipov, 2003; Schutt et al., 1996; Styler et al., 2009). Styler et al. (2009)

* Corresponding author. Tel.: +86 10 62849123; fax: +86 10 62923563.
E-mail address: honghe@rcees.ac.cn (H. He).

1352-2310/$ – see front matter
http://dx.doi.org/10.1016/j.atmosenv.2013.02.039

found the reaction between solid pyrene surface and ozone was enhanced in the presence of near-UV radiation (300–420 nm). However, the effect of visible irradiation (400–700 nm) on the heterogeneous ozonation of PAHs was not clear at present. In the present work, the heterogeneous reactions of gas-phase ozone with anthracene adsorbed on mineral dust particles in presence and absence of visible light were studied using attenuated total reflection Fourier transform infrared (ATR-FTIR) and gas chromatography mass spectrometry (GC–MS) technique. The results will help for understanding the chemical behaviour of PAHs in the atmosphere.

2. Experimental

2.1. Sampling and particles characterization

TiO_2, although being a minor component of mineral dust particles (Karagulian et al., 2006), was shown recently to be responsible for the photochemical reactivity of atmospheric mineral aerosols (Ndour et al., 2008). Therefore, it was chosen as the model particles of mineral dust. TiO_2 was purchased from commercial sources (Degussa P25, $S_{BET} = 50\ m^2\ g^{-1}$). Asian dust storm particles were collected in a clean jar on the roof of a building (about 20 m high) of the Research Center of Eco-Environmental Sciences, CAS (116.3° E, 39.9° N, Beijing), on 16–17 April 2006, during a heavy dust storm. The size distribution measured by laser size analysis showed that the $d_{0.5}$ of the particles was 20 μm. The BET area determined from nitrogen adsorption–desorption isotherms at 77 K using Nitrogen Brunauer–Emmett–Teller (BET) physisorption (Micromeritics ASAP 2000) was 5.43 $m^2\ g^{-1}$.

2.2. Sample preparation and storage

Before adsorption of PAHs, particles were cleaned three times by ultrasonication in the mixture of dichloromethane and n-hexane (Chromatographic Grade), followed by drying at room temperature. The concentration of PAHs in the extract of cleaned particles and the pure solvent can not be detected by the gas chromatography–mass spectrometer (Agilent 6890/5973).

Anthracene was adsorbed on particles by the impregnation method. Approximately 1.0 g of cleaned dust particles was added to 20.0 mL of n-hexane containing 500 μg of anthracene. Approximately 0.1 g of cleaned TiO_2 particles was added to 20.0 mL of n-hexane containing 5 mg of anthracene. After stirred homogeneously, the solvent was slowly evaporated using a rotary evaporator at 303 K. Finally, the particles were dried at room temperature for 4 h. To avoid the photodegradation of adsorbed PAHs, all particles were stored in amber glass flasks at 255 K in the dark.

2.3. O_3 generation and detection

O_3 was generated by a homemade quartz O_3 generator, in which a mixed flow of dry O_2 and N_2 was irradiated by a mercury lamp with wavelength of 185 and 254 nm. The concentration of O_3 in the feed gas was controlled by varying the ratio of O_2 to N_2 passing through the mercury lamp and was detected by an O_3 monitor (Model 202, 2B Technology).

2.4. In situ attenuated total reflection Fourier transform infrared (ATR-FTIR)

The IR spectra were recorded on a NEXUS 6700 (Thermo Nicolet Instrument Corporation) FTIR, equipped with a homemade *in situ* attenuated total reflection Fourier transform infrared (ATR-FTIR) and a MCT detector. All experiments were performed at 293 K. The coated TiO_2 sample was suspended in distilled water at a concentration of 1 mg mL^{-1}. The suspension was treated for 10 min in an ultrasonic bath; 1 mL of this suspension was spread on the ZnSe crystal and purged with N_2 overnight to remove water. The total flow rate was 100 mL min^{-1}, and the concentration of O_3 was 2 ppm. The light was obtained by a 500 W xenon lamp (Beijing TrusTech Science and Technology Co., China) equipped with a liquid light guide and quartz lens. The radiant flux density was measured with a radiometer (Photoelectric Instrument Factory of Beijing Normal University). The light intensity was 25 mw cm^{-2} during the experiment. Temperature changes for the reactor, measured by a thermocouple, were typical 5 K. The ZeSe crystal is used as the background to get the absorption spectra. The reference spectrum was measured in a synthesized air stream at 293 K. All spectra reported were recorded at a resolution of 4 cm^{-1} for 100 scans.

2.5. Gas chromatography–mass spectrometry (GC–MS)

All experiments were performed at 298 K. A total of 20.0 mg of coated particles were evenly deposited on a Teflon disc (the geometric surface area is 3.39 cm^2), which was then placed in a quartz reactor. Before O_3 was introduced into the quartz reactor, $O_2/O_3/N_2$ of a given concentration was flowed through another blank reactor. When the concentration of O_3 was stable, the feed gas was switched to the reactor containing adsorbed PAHs for reaction. In another independent experiment, particles were simultaneously exposed to O_3 and irradiated with simulated sunlight emitted from a 500 W xenon lamp (Beijing TrusTech Science and Technology Co., China) at a distance of 13 cm from the reactor. The light intensity was also 25 mw cm^{-2} during the experiment. Temperature changes for the flow reactor, measured by a thermocouple, were typical 1 K.

The reacted particle samples were ultrasonically extracted using 20.0 mL CH_2Cl_2 and were then filtered using a glass fibre filter, which had been previously cleaned in the same manner as the pure mineral oxides. Subsequently, CH_2Cl_2 was evaporated and changed to 1.00 mL n-hexane under a gentle stream of nitrogen gas at 293 K.

Analyses of PAHs samples were performed by a GC–MS. The column was a HP 5MS (30 m × 0.25 mm i.d. × 0.25 μm film thickness). The methodology for the analysis of PAHs is similar to our previous study (Ma et al., 2010, 2011). The concentration of PAHs in solution were measured based on an external standard and the use of a calibration curve. The recovery obtained from spike and recovery experiments for anthracene on dust particles was (99.6 ± 6.27)%. Therefore, GCMS areas were corrected for 100% recovery before quantification with the calibration curve.

2.6. Chemicals

All chemicals were chromatographic grade and used without further purification. CH_2Cl_2 and n-hexane were obtained from Baker Analyzed and Dima Technology Inc. Anthracene (99%) and anthraquinone (99.5%) were purchased from Acros Organics and Dr. Ehrenstorfer GmbH. Polynuclear aromatic hydrocarbon mix (the purity of anthracene is 100% and the prepared and certified analyte concentration of anthracene is 100 and 100.3 μg mL^{-1}, respectively), which was used as the standard for calibrations, was purchased from AccuStandard, Inc. High purity N_2 and O_2 were supplied by Beijing AP BEIFEN Gases Inc.

3. Results and discussion

3.1. Blank experiment

Since ZnSe crystal is the optical lens of ATR and an inert material, the heterogeneous reaction between O_3 and anthracene on it

was regarded as that of the heterogeneous reaction between O_3 and pure anthracene particles. Firstly, the interaction between anthracene and N_2 was investigated in the absence and presence of light. The infrared spectra of pure anthracene particles and dynamic changes of the averaged integrated area of anthracene on ZnSe in a flow of 100 mL min^{-1} dry N_2 are shown in Figs. S.1 and S.2. The intensity of bands assigned to anthracene decreased slightly under dark conditions, while the intensity of bands assigned to anthracene decreased evidently in the presence of light. No product peaks were observed in the absence and presence of light. Therefore, it can be attributed to the volatilization of anthracene from ZnSe surface. More amount of anthracene volatilized from ZnSe surface in the presence of light may be due to the slightly elevated of temperature or light induced nonthermal desorption.

In situ ATR-FTIR spectra of anthracene on ZnSe exposed to O_3 or O_3/light with synthetic air are displayed in Fig. 1. The bands at 3048, 957, 855 and 726 cm^{-1} are the characteristic feature of anthracene (Fig. 1A and B). The heterogeneous reaction between anthracene and O_3 in the dark was slow, however, this reaction displayed a light enhancement. As shown in Fig. 1C, several bands at 1776, 1715, 1679, 1591, 1336 and 1288 cm^{-1} were observed in the spectra. The bands at 1679, 1591, 1336 and 1288 cm^{-1} are attributed to the C═O stretching, C═C stretching, C–C stretching and ring deformation of 9,10-anthraquinone, respectively (Ball et al., 1996). The bands at 1776 and 1715 cm^{-1} can be assigned to the C═O stretching of phthalic anhydride. These results indicate that anthracene can react with O_3 to form anthraquinone in the dark. Anthraquinone can further react in the presence of light.

The dynamic changes of the integrated area of anthracene under different conditions were shown in Fig. 2. The reaction between O_3 and pure anthracene particles in the dark was slow but the reaction exhibited an exponential behaviour in the presence of light. This means that light can promote the reaction between O_3 and pure anthracene particles.

3.2. Heterogeneous reaction between ozone and anthracene adsorbed on TiO_2

Heterogeneous reaction between O_3 and anthracene adsorbed on TiO_2 was obviously faster than reaction between O_3 and pure anthracene particles. The dynamic changes of the integrated area of anthracene under different conditions were shown in Fig. 3. The volatilization of anthracene on TiO_2 was neglectable in the dark. This means that the interaction between anthracene and TiO_2 was strong. When the light was introduced to the reactor, the consumption of anthracene in a flow of dry N_2 was more evident than that on ZnSe. Additionally, no product peaks was observed in the spectra (data not shown). Dabestani et al. (1995) proposed that anthracene can photo-dimerization on dry surface of SiO_2 and Al_2O_3 in the absence of oxygen. Therefore, the consumption of anthracene can be attributed to the volatilization and photo-dimerization of anthracene on TiO_2 in the presence of light. The heterogeneous reaction between O_3 and anthracene on TiO_2 was obviously faster than that on ZnSe in the dark. This suggests that the reactivity of anthracene with O_3 is determined by the nature of the substrate. The concentration of anthracene was steady after

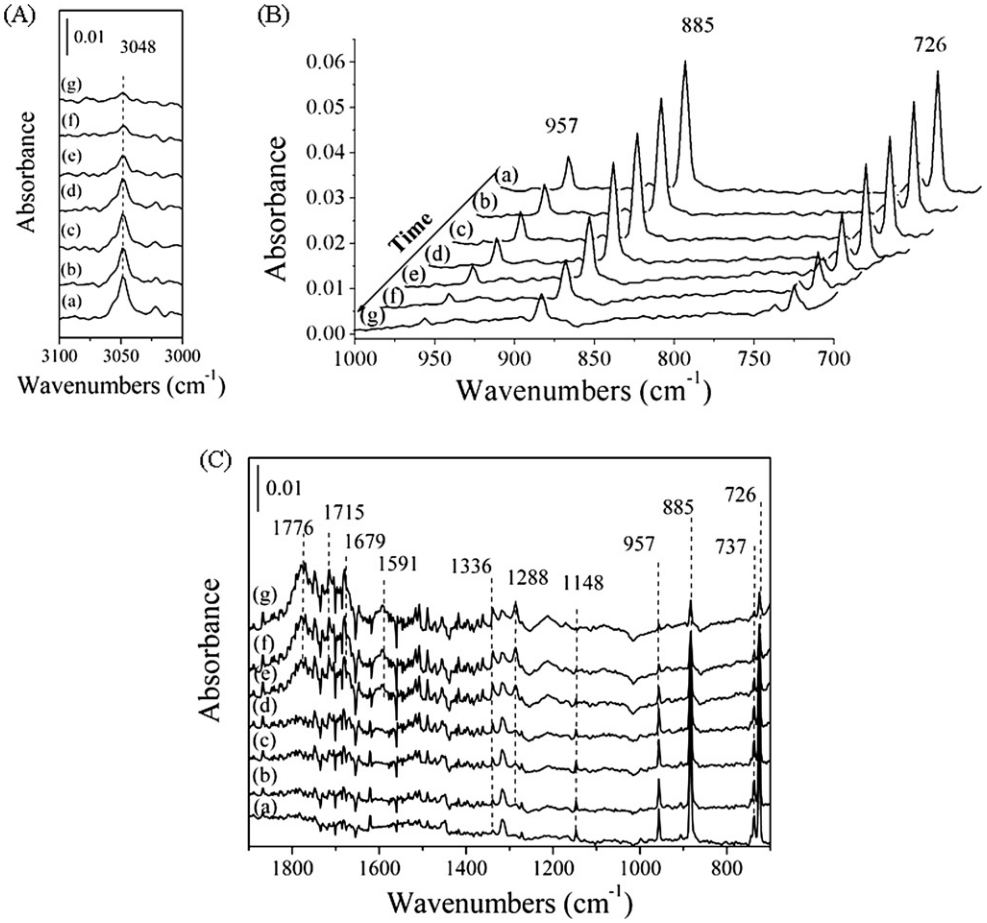

Fig. 1. Dynamic changes of *in situ* ATR-FTIR spectra for anthracene on ZnSe in a flow of 100 mL min^{-1} 2 ppmv O_3 + air (a) O_3 0 h; (b) O_3 1 h; (c) O_3 2 h; (d) O_3 3 h; (e) Light 1 h; (f) Light 2 h; (g) Light 3 h.

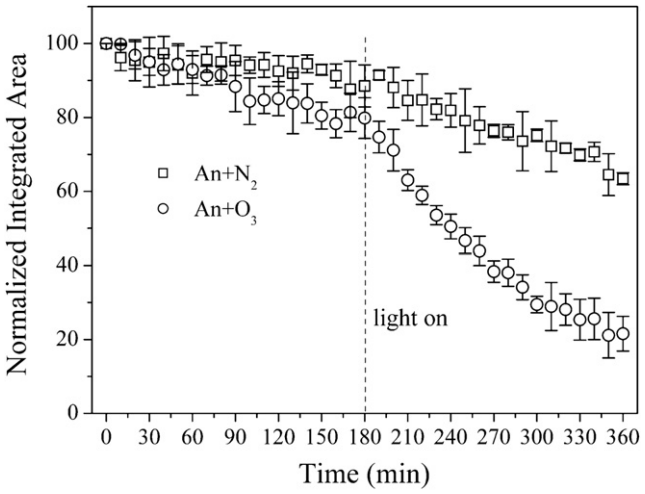

Fig. 2. Dynamic changes of the integrated area of anthracene on ZnSe under different conditions.

three hours of dark reaction, but anthracene can be further consumed in the presence of light (Fig. 3).

In situ ATR-FTIR spectra of anthracene on TiO_2 exposed to O_3 or O_3/light with synthetic air are displayed in Fig. S.3. The dynamic changes of the integrated area of anthracene and anthraquinone on TiO_2 in a flow of 100 mL min^{-1} 2 ppmv O_3 + air were shown in Fig. 4. With the reaction proceeding, the integrated area of anthracene decreased while the integrated area of anthraquinone increased in the dark. When the light was introduced to the reactor, integrated area of anthraquinone decreased immediately. Blank experiments indicate that the decay of anthraquinone on TiO_2 in the presence of light was not attributed to the increase of temperature (Fig. S.4). These results suggest that anthraquinone can react with O_3 quickly in the presence of light.

Because of the fast reaction between O_3 and anthracene adsorbed on TiO_2 in the dark, anthracene was almost consumed completely after 3 h. The effect of light on the heterogeneous reaction between O_3 and anthracene adsorbed on TiO_2 was further investigated. Fig. 5 shows the dynamic changes of the integrated area of anthracene on TiO_2 in 100 mL min^{-1} 2 ppmv O_3 in synthetic air in the absence and presence of light. The heterogeneous reaction between O_3 and anthracene adsorbed on TiO_2 displayed a light enhancement. Under the assumption of linearly relations between

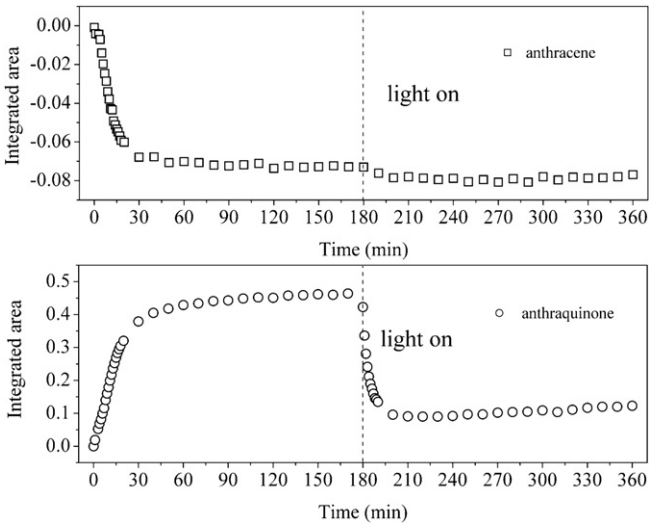

Fig. 4. Dynamic changes of the integrated area of anthracene and anthraquinone on TiO_2 in a flow of 100 mL min^{-1} 2 ppmv O_3 + air.

the concentration of anthracene and the integrated area of anthracene, the estimated reaction rate constants was increased by a factor of 1.5 in the presence of light. Additionally, the reaction extent was promoted by light.

3.3. Heterogeneous reaction kinetics between ozone and anthracene adsorbed on Asian dust storm particles

As discussed above, the ozonation rate of PAHs is highly influenced by the nature of the substrate. Therefore, Asian dust storm particles were chose as substrate to investigate the heterogeneous reaction of anthracene with O_3. Anthraquinone was identified as the main surface product of anthracene reacted with ozone (Fig. S.5). The kinetics of the heterogeneous reaction between O_3 and anthracene adsorbed on Asian dust storm particles were determined by monitoring the loss of anthracene as a function of O_3 exposure time at 298 K. The degradation of anthracene on Asian dust storm particles showed an exponential pattern (Fig. 6), which suggests that the reactions are reasonably described by pseudo-first-order kinetics. Therefore, the experimental data were fitted using pseudo-first-order exponential functions shown in equation (1),

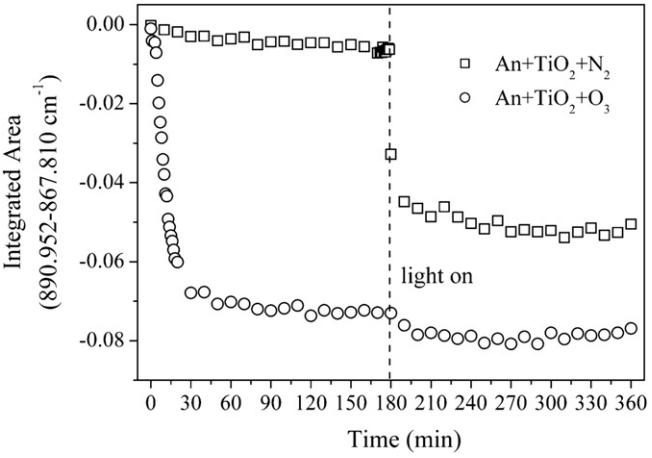

Fig. 3. Dynamic changes of the integrated area of anthracene on TiO_2 in a flow of 100 mL min^{-1} dry N_2 or 2 ppmv O_3 + air.

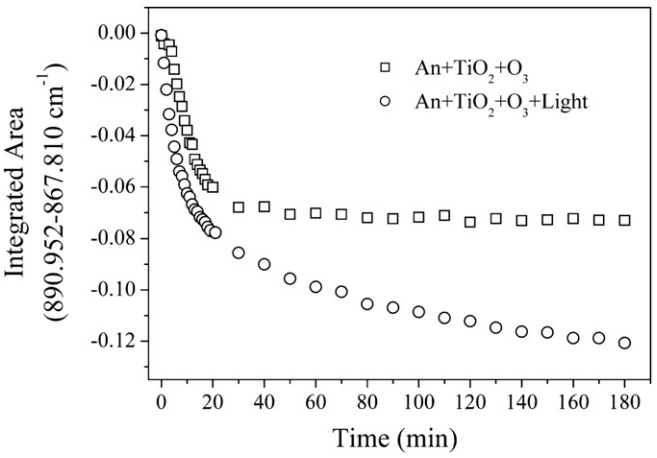

Fig. 5. Dynamic changes of the integrated area of anthracene on TiO_2 in a flow of 100 mL min^{-1} 2 ppmv O_3 + air.

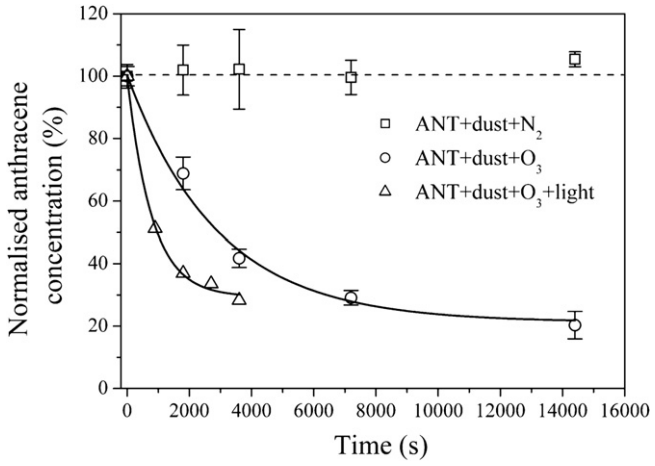

Fig. 6. The change of normalized concentration of anthracene adsorbed on Asian dust storm particles under different conditions at 298 K: (□) in N_2 flow, (○) ~ 1.37×10^{14} molecules cm^{-3} O_3 in the absence of light, (△) ~ 1.37×10^{14} molecules cm^{-3} O_3 in the presence of light.

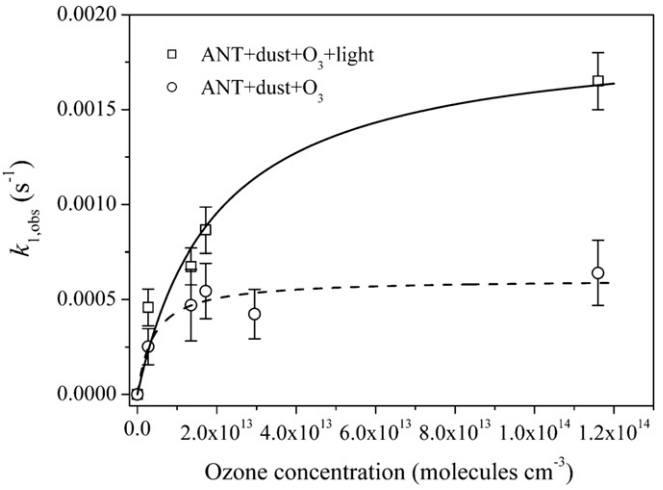

Fig. 7. Pseudo-first-order rate constants ($k_{1,obs}$) as a function of gas-phase O_3 concentration for the reactions of O_3 and anthracene adsorbed on Asian dust storm particles (○) under dark conditions, (□) under solar light irradiation. The dashed line and solid line represent the fit of the experimental observations to the modified Langmuir–Hinshelwood mechanism (Eq. (3)).

$$\frac{[PAH]_t}{[PAH]_0} = \frac{[PAH]_{plateau}}{[PAH]_0} + \frac{[PAH]_0 - [PAH]_{plateau}}{[PAH]_0} \times \exp(-k_{1,obs} \times t) \quad (1)$$

where $[PAH]_t$ is the concentration of adsorbed PAH at a given time, $[PAH]_0$ is the initial concentration of adsorbed PAH, $[PAH]_{plateau}$ is the concentration of adsorbed PAH at the plateau shown in Fig. 6, and $k_{1,obs}$ is the apparent rate constant of the pseudo-first-order reaction. The $k_{1,obs}$ values were $(3.52 \pm 0.53) \times 10^{-4}$ s^{-1} and $(1.29 \pm 0.13) \times 10^{-3}$ s^{-1} in the absence and presence of light, respectively. The reaction rate in the presence of light was almost four times faster than that in the absence of light. The values of $k_{1,obs}$ was 2 orders of magnitude lower than that on SiO_2, α-Al_2O_3 and α-Fe_2O_3 measured under similar conditions (in the absence of light) (Ma et al., 2010). Many hypotheses were put forward to explain these phenomena. One possibility is that Asian dust storm particles were aged in the atmosphere or the structures of dust particles were different with that of mineral oxides. Additionally, the reaction between O_3 and anthracene on other component of Asian dust storm particles except SiO_2, α-Al_2O_3 and α-Fe_2O_3 may be slow. As can be seen in Fig. 6, the degradation of PAHs reached a plateau on Asian dust storm particles, which suggested that the anthracene was not being deposited as a smooth, uniform layer, but more likely as clumps or islands.

In previous study, we found the reaction between O_3 and anthracene adsorbed on SiO_2, α-Al_2O_3 and α-Fe_2O_3 proceeds by the Langmuir–Hinshelwood mechanism (Ma et al., 2010). In order to clarify the surface reaction mechanism of O_3 with anthracene adsorbed on Asian dust storm particles, the $k_{1,obs}$ at different gas-phase O_3 concentrations were measured. As shown in Fig. 7, the plot of $k_{1,obs}$ is nonlinearly related to gas-phase O_3 concentration, which is consistent with the modified Langmuir–Hinshelwood reaction mechanism. This mechanism involves the reaction of surface species in which one reactant (i.e. the PAHs) is adsorbed on the particle surface while a second reactant (i.e. O_3) is in equilibrium between the gas phase and the surface. The surface reaction takes place between two adsorbed species on the surface of the substrates. This kind of mechanism was observed for the reaction between surface-bound PAHs and O_3 on different substrates (Kahan et al., 2006; Kwamena et al., 2006, 2007, 2004; Ma et al., 2010; Mmereki et al., 2004; Pöschl et al., 2001).

In the modified Langmuir–Hinshelwood mechanism, the $k_{1,obs}$ can be interpreted as (Kahan et al., 2006; Kwamena et al., 2006, 2007, 2004; Mmereki and Donaldson, 2003; Mmereki et al., 2004; Pöschl et al., 2001, 2007)

$$k_{1,obs} = \frac{k_2[SS]_s K_{O_3}[O_3]_g}{1 + K_{O_3}[O_3]_g} \quad (2)$$

where $[SS]_s$ is the surface concentration of ozone adsorption sites, K_{O_3} is the Langmuir adsorption equilibrium constant for O_3, i.e. the ratio of rate constants between the adsorption and desorption of O_3 ($k_{a,O_3}/k_{d,O_3}$), $[O_3]_g$ is the gas-phase concentration of O_3. From this equation, it is evident that $k_{1,obs}$ is dependant on both the number of surface sites and the gas-phase concentration of O_3. The $k_2[SS]_s$ represents the maximum pseudo-first-order rate constant of anthracene at high O_3 concentration ($\theta_{O_3} \to 1$), and is replaced with $k_{1,max}$. Then equation (2) can be rewritten as (Kwamena et al., 2006, 2007, 2004)

$$k_{1,obs} = \frac{k_{1,max} K_{O_3}[O_3]_g}{1 + K_{O_3}[O_3]_g} \quad (3)$$

Fig. 7 shows the fitting curves based on equation (3) using nonlinear least-squares fitting. The fitting parameters, including K_{O_3} and $k_{1,max}$ are listed in Table 1. The errors for these parameters were obtained from the statistical errors of the nonlinear least-squares fitting.

The fitting parameters (K_{O_3} and $k_{1,max}$) for the reactions between O_3 and anthracene adsorbed on Asian dust storm particles are summarized in Table 1.

At an atmospherically relevant ozone mixing ratio of about 60 ppb, the first order rate constant of anthracene degradation at the Asian dust storm particles surface is 1.48×10^{-4} s^{-1} in the

Table 1
Kinetic parameters for the reaction of ozone with anthracene adsorbed on Asian dust storm particles under different conditions.

Conditions	$k_{1,max}$ (10^{-3} s^{-1})	K_{O_3} (10^{-13} cm^3)
Dark	0.61 ± 0.06	3.30 ± 1.62
Light	1.91 ± 0.24	0.57 ± 0.20

presence of light. At extremely high ozone concentrations (see the plateau in Fig. 7), the degradation of anthracene is enhanced by a factor of 3 in the presence light compared to the dark conditions.

4. Conclusions

In this study, heterogeneous reactions of O_3 with anthracene adsorbed on TiO_2 and Asian dust storm particles were investigated in the presence and absence of light at room temperature. The consumption of anthracene on TiO_2 in a flow of dry N_2 in the presence of light may be caused by the volatilization and photodimerization. The ozonation products of anthracene (anthraquinone) can react with O_3 quickly in the presence of light. The reaction rate constants on TiO_2 were increased by a factor of 1.5 in the presence of light.

The values of $k_{1,obs}$ for heterogeneous reaction between O_3 and anthracene adsorbed on Asian dust storm particles was 2 orders of magnitude lower than that on SiO_2, α-Al_2O_3 and α-Fe_2O_3 measured under dark conditions. This work showed that the reactions between ozone and anthracene adsorbed on Asian dust storm particles proceed by the Langmuir–Hinshelwood mechanism in the dark and in the presence of light. At extremely high ozone concentrations, the degradation of anthracene is enhanced by a factor of 3 in the presence of light compared to the dark conditions. Thus, heterogeneous photochemical reaction of ozone with anthracene adsorbed on mineral dust needs to be considered into accurate models for estimation the reactive fate of PAHs in the atmosphere.

Acknowledgements

This research was funded by the National Natural Science Foundation of China (20937004, 51221892) and the Strategic Priority Research Program of the Chinese Academy of Sciences (No. XDB05050600).

Appendix A. Supplementary data

Supplementary data related to this article can be found at http://dx.doi.org/10.1016/j.atmosenv.2013.02.039.

References

Ball, B., Zhou, X.F., Liu, R.F., 1996. Density functional theory study of vibrational spectra .8. Assignment of fundamental vibrational modes of 9,10-anthraquinone and 9,10-anthraquinone-d_8. Spectrochimica Acta Part A 52, 1803–1814.

Barbas, J.T., Dabestani, R., Sigman, M.E., 1994. A mechanistic study of photodecomposition of acenaphthylene on a dry silica surface. Journal of Photochemistry and Photobiology A: Chemistry 80, 103–111.

Behymer, T.D., Hites, R.A., 1985. Photolysis of polycyclic aromatic hydrocarbons adsorbed on simulated atmospheric particulates. Environmental Science and Technology 19, 1004–1006.

Bernstein, M.P., Sandford, S.A., Allamandola, L.J., Gillette, J.S., Clemett, S.J., Zare, R.N., 1999. UV irradiation of polycyclic aromatic hydrocarbons in ices: production of alcohols, quinones, and ethers. Science 283, 1135–1138.

Cope, V.W., Kalkwarf, D.R., 1987. Photooxidation of selected polycyclic aromatic hydrocarbons and pyrenequinones coated on glass surfaces. Environmental Science and Technology 21, 643–648.

Dabestani, R., Ellis, K.J., Sigman, M.E., 1995. Photodecomposition of anthracene on dry surfaces: products and mechanism. Journal of Photochemistry and Photobiology A: Chemistry 86, 231–239.

Dunstan, T.D.J., Mauldin, R.F., Jinxian, Z., Hipps, A.D., Wehry, E.L., Mamantov, G., 1989. Adsorption and photodegradation of pyrene on magnetic, carbonaceous, and mineral subfractions of coal stack ash. Environmental Science and Technology 23, 303–308.

Finlayson-Pitts, B.J., Pitts, J.-N., 1997. Tropospheric air pollution: ozone, airborne toxics, polycyclic aromatic hydrocarbons, and particles. Science 276, 1045–1052.

Fioressi, S., Arce, R., 2005. Photochemical transformations of benzo[e]pyrene in solution and adsorbed on silica gel and alumina surfaces. Environmental Science and Technology 39, 3646–3655.

Fox, M.A., Olive, S., 1979. Photooxidation of anthracene on atmospheric particulate matter. Science 205, 582–583.

Gloaguen, E., Mysak, E.R., Leone, S.R., Ahmed, M., Wilson, K.R., 2006. Investigating the chemical composition of mixed organic–inorganic particles by "soft" vacuum ultraviolet photoionization: the reaction of ozone with anthracene on sodium chloride particles. International Journal of Mass Spectrometry 258, 74–85.

Kahan, T.F., Kwamena, N.O.A., Donaldson, D.J., 2006. Heterogeneous ozonation kinetics of polycyclic aromatic hydrocarbons on organic films. Atmospheric Environment 40, 3448–3459.

Karagulian, F., Santschi, C., Rossi, M.J., 2006. The heterogeneous chemical kinetics of N_2O_5 on $CaCO_3$ and other atmospheric mineral dust surrogates. Atmospheric Chemistry and Physics 6, 1373–1388.

Korfmacher, W.A., Wehry, E.L., Mamantov, G., Natusch, D.F.S., 1980. Resistance to photochemical decomposition of polycyclic aromatic hydrocarbons vapor-adsorbed on coal fly ash. Environmental Science and Technology 14, 1094–1099.

Kwamena, N.O.A., Earp, M.E., Young, C.J., Abbatt, J.P.D., 2006. Kinetic and product yield study of the heterogeneous gas-surface reaction of anthracene and ozone. Journal of Physical Chemistry A 110, 3638–3646.

Kwamena, N.O.A., Staikova, M.G., Donaldson, D.J., George, I.J., Abbatt, J.P.D., 2007. Role of the aerosol substrate in the heterogeneous ozonation reactions of surface-bound PAHs. Journal of Physical Chemistry A 111, 11050–11058.

Kwamena, N.O.A., Thornton, J.A., Abbatt, J.P.D., 2004. Kinetics of surface-bound benzo[a]pyrene and ozone on solid organic and salt aerosols. Journal of Physical Chemistry A 108, 11626–11634.

Ma, J.Z., Liu, Y.C., He, H., 2010. Degradation kinetics of anthracene by ozone on mineral oxides. Atmospheric Environment 44, 4446–4453.

Ma, J.Z., Liu, Y.C., He, H., 2011. Heterogeneous reactions between NO_2 and anthracene adsorbed on SiO_2 and MgO. Atmospheric Environment 45, 917–924.

Matsuzawa, S., Nasser-Ali, L., Garrigues, P., 2001. Photolytic behavior of polycyclic aromatic hydrocarbons in diesel particulate matter deposited on the ground. Environmental Science and Technology 35, 3139–3143.

Mmereki, B.T., Donaldson, D.J., 2003. Direct observation of the kinetics of an atmospherically important reaction at the air–aqueous interface. Journal of Physical Chemistry A 107, 11038–11042.

Mmereki, B.T., Donaldson, D.J., Gilman, J.B., Eliason, T.L., Vaida, V., 2004. Kinetics and products of the reaction of gas-phase ozone with anthracene adsorbed at the air–aqueous interface. Atmospheric Environment 38, 6091–6103.

Ndour, M., D'Anna, B., George, C., Ka, O., Balkanski, Y., Kleffmann, J., Stemmler, K., Ammann, M., 2008. Photoenhanced uptake of NO_2 on mineral dust: laboratory experiments and model simulations. Geophysical Research Letters 35, L05812.

Pöschl, U., Letzel, T., Schauer, C., Niessner, R., 2001. Interaction of ozone and water vapor with spark discharge soot aerosol particles coated with Benzo[a]pyrene: O_3 and H_2O adsorption, benzo[a]pyrene degradation, and atmospheric implications. Journal of Physical Chemistry A 105, 4029–4041.

Pöschl, U., Rudich, Y., Ammann, M., 2007. Kinetic model framework for aerosol and cloud surface chemistry and gas-particle interactions – part 1: general equations, parameters, and terminology. Atmospheric Chemistry and Physics 7, 5989–6023.

Pitts Jr., J.N., Lokensgard, D.M., Ripley, P.S., van Cauwenberghe, K.A., Van Vaeck, L., Shaffer, S.D., Thill, A.J., Belser, W.L., 1980. "Atmospheric" epoxidation of benzo[a]pyrene by ozone: formation of the metabolite benzo[a]pyrene-4,5-oxide. Science 210, 1347–1349.

Prokopenko, S.L., Osipov, V.V., 2003. Photoozonolysis of anthracene and eosin at the surface of SiO_2. Theoretical and Experimental Chemistry 39, 347–351.

Schutt, W.S., Sigman, M.E., Li, Y.Z., 1996. Fluorimetric investigation of reactions between ozone and excited state aromatic compounds on silica gel. Analytica Chimica Acta 319, 369–377.

Styler, S.A., Brigante, M., D'Anna, B., George, C., Donaldson, D.J., 2009. Photoenhanced ozone loss on solid pyrene films. Physical Chemistry Chemical Physics 11, 7876–7884.

Wang, D.G., Chen, J.W., Xu, Z., Qiao, X.L., Huang, L.P., 2005. Disappearance of polycyclic aromatic hydrocarbons sorbed on surfaces of pine *Pinua thunbergii* needles under irradiation of sunlight: volatilization and photolysis. Atmospheric Environment 39, 4583–4591.